inventions

MDPI

Technical Note

Fully-Programmable, Low-Cost, "Do-It-Yourself" Pressure Source for General Purpose Use in the Microfluidic Laboratory

Philipp Frank [1,2], Sebastian Haefner [1,2], Martin Elstner [3] and Andreas Richter [1,2,3,*]

[1] Polymeric Microsystems, Institute for Semiconductors and Microsystems, Technische Universität Dresden, Nöthnitzer Street 64, 01062 Dresden, Germany; philipp.frank@tu-dresden.de (P.F.); sebastian.haefner@tu-dresden.de (S.H.)

[2] Research Training Group 1865 "Hydrogel-Based Microsystems", German Research Foundation, 01062 Dresden, Germany

[3] Center for Advancing Electronics Dresden (CFAED), 01062 Dresden, Germany; martin.elstner@tu-dresden.de

* Correspondence: andreas.richter7@tu-dresden.de; Tel.: +49-351-463-36336

Academic Editor: Chien-Hung Liu
Received: 28 April 2016; Accepted: 16 June 2016; Published: 22 June 2016

Abstract: Microfluidics is still a fast growing field and an interesting market, which increasingly demands sophisticated equipment and specific engineering solutions. Aside from the widely discussed chip technology, the external equipment and machinery to operate such a microfluidic chip system comes into focus. A number of companies offer solutions to pursue the various requests made by the microfluidic community. Commercially available systems for pumping fluids are versatile but also highly expensive. Here, we present a fully-programmable pressure source, which is low-cost and can be utilized for pressure-controlled fluid driving, destructive bonding tests, and other pressure-relevant experiments. We evaluated our setup and compared the performance to a commercially available system. Furthermore, we demonstrated the use of the system in the field of droplet microfluidics as a possible application. Our development aims to lower the entrance threshold for microfluidic technology and make it more accessible to a broader audience.

Keywords: microfluidics; pressure source; pressure-driven flow; precision instruments; laboratory equipment; do-it-yourself

1. Introduction

Microfluidics have emerged to become the enabler technology in the fields of biology, biochemistry and life sciences [1–5]. As the microfluidic community grows larger, the requirement for sophisticated equipment and individual engineering solutions also arises. Microfluidic chip technology [6–10] and rapid prototyping strategies [11–14] have been widely covered over the last two decades. Besides the microfluidic chip, the external equipment to operate the devices and to drive fluids gain more and more importance. Basically, two types of pumps for displacing fluid and supplying the microfluidic chips can be distinguished. The first type is a flow-controlled pump, which commonly is implemented by syringe pumps. The principle is to unload a syringe using a precision stepping motor and a transmission steadily pressing the piston of the syringe. The flow-controlled pumps put out a constant liquid flow, which depends on the cross-section of the syringe and the velocity of the piston being moved. The second type is a pressure-controlled pump, which is popular especially when using electronic-like analogies to calculate microfluidic networks [15–17]. The most straightforward way to realize such a pressure-controlled pump is by hydrostatic pressure. A column of water is set up,

where a liquid reservoir connected downward to a tube is set at a certain height. The height difference between the reservoir and the tube outlet results in the hydrostatic pressure given through Equation (1):

$$p = \rho \cdot g \cdot \Delta h. \quad (1)$$

where p is the pressure, ρ is the density of the medium, g is the gravitational acceleration and Δh is the height difference.

The hydrostatic pressure pump is low cost and functions without auxiliary power, though is bound to certain limitations. This passive device is not programmable and the maximum pressure is limited to the maximum height difference (see Equation (1)) reached, resulting in a rather bulky setup. Commercially available pressure-controlled pumps are programmable and utilize air compressors and controllers to set the pressure in a closed container holding the liquid. Typically, the lit of the container has two connectors, one to apply the pressure via pressurizing air and another one for the liquid tube to exit. While the overall dispensed volume and precision of a syringe pump is limited by the syringe size, a pressure pump can dispense virtually any volume size only depending on the used fluid container. Although professional equipment exists for both flow and pressure driven pumps, these commercial systems are also highly expensive and restricted in their modular expandability, hindering individual customization. Here, we present a fully programmable and inexpensive pressure source, which is highly flexible, easily customized and can be extended to the individual needs of any application, on the hardware side as well on the software side. The system requires a small amount of financial effort to be implemented and is easily maintained. The setup is assembled from low-cost components and is do-it-yourself (DIY) in nature. The implementation of the system is straightforward and well-suited for automation purposes. The setup can be achieved without the requirements of specific training or equipment. The software developed to operate the components is provided in the supplement. We show that the DIY pressure source is capable of functioning as a pressure-controlled pump. The approach aims to lower the entrance barrier for microfluidic technology and make sophisticated pumping modules accessible to a broader audience. We also want to contribute to the DIY concept as it has been strongly established within the microfluidic community [18,19]. In our studies, we characterized our setup and compared it to a commercially available pumping system. The accuracy, precision, noise and hysteresis systems are compared, respectively. In order to demonstrate the capability of the system, we show a possible application in the field of droplet microfluidics. Within the experiment, we generate water-in-oil droplets over a series of different ratios of the two pressure-driven phases.

2. Materials and Methods

2.1. Concept

The central unit of the programmable pressure source is an industrial pressure controller (ITV0010-2UBL, SMC, Tokyo, Japan) supplying an output pressure range from 0.01 mbar to 1000 mbar. The pressure controller requires an external source of compressed air and is operated over an electrical analog volt signal. The schematic of the system can be seen in Figure 1. The fieldbus system generated the electrical signal (0 V to 5 V) for the controller and simultaneously monitored the internal pressure signal (1 V to 5 V) of the controller. The fieldbus system (750–881, WAGO GmbH, Minden, Germany) was equipped with a 12-bit analog output clamp (750–559, WAGO GmbH) and a 12-bit analog input clamp (750–468, WAGO GmbH). The communication between fieldbus and computer was conducted via ethernet and a python-based software (Python 2.7.9) utilizing the python module *PyModbus* and an according graphical user interface (GUI).

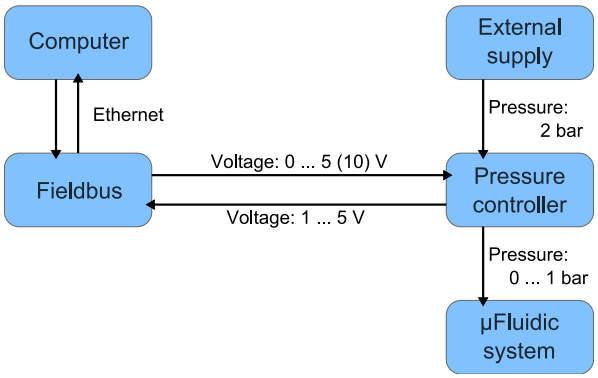

Figure 1. Basic concept of the proposed pressure source. The electronic control is embodied by a fieldbus and a pressure controller fed by an external supply of pressured air. The fieldbus system facilitates the electrical control signals to the pressure controller and reads back the internal sensor signal of the pressure controller.

2.2. Characterization Setup

The setup to characterize the pressure source can be seen in Figure 2. The pressure source was tested for two cases. In the first case, the pressure source was solely connected to a pressure sensor (PD23, Keller, Winterthur, Switzerland) without a load of a microfluidic system ($R = \infty$); hence, no flow was generated. In the second case of testing, a microfluidic system including a flow sensor (Flow sensor 0182, Gesim mbH, Radeberg, Germany) was additionally connected to the pressure source to mimic real-world conditions. The hydraulic resistance of the fluidic system was varied (R_H = 35.8, 20.0 and 11.0 mbar min µL^{-1}). The target value was the pressure at the source, which was measured by the pressure sensor. The pressure sensor was also evaluated with a 12-bit AD-converter clamp (750–468, WAGO GmbH) mounted on the fieldbus. The testing routine was a step function from 0 mbar pressure up 1000 mbar in steps of 25 mbar. Each step was held for 10 s and was repeated when the step function was reversed from 1000 mbar down to 0 mbar. The routine was repeated twice. For reference, we also tested a commercially available pressure pump and compared the data with our setup. Figure S1 in the supplement provides an overview photograph of the experimental setup and Figure S2 holds detailed information about the microfluidic chip system. The commercial pump was the AF1 microfluidic pressure pump (Elveflow Instruments, Paris, France).

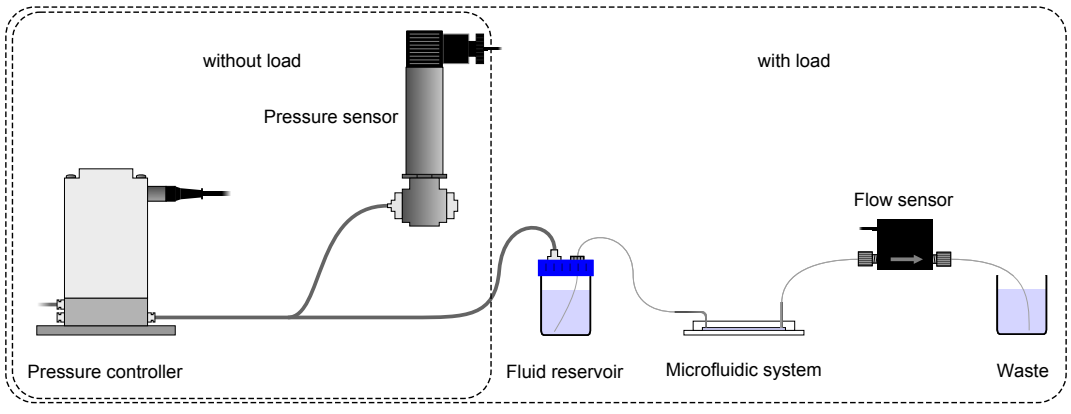

Figure 2. Characterization setup for pressure source. Without load: pressure source solely connected to the pressure sensor, no flow generated. With load: pressure source connected to the pressure sensor and a microfluidic system and a flow sensor over a V-connector. The hydraulic resistance of the microfluidic system was varied between R_H = 35.8, 20.0 and 11.0 mbar min µL^{-1}.

2.3. Microfluidic Chip System

2.3.1. Master Fabrication

A glass substrate (26 mm × 76 mm, Menzel-Gläser, Gerhard Menzel B.V. & Co.KG, Braunschweig, Germany) with a thickness of 1.0 mm was cleaned with acetone, isopropanol and de-ionized water and dried using nitrogen. Consecutively, a dehydration bake at 150 °C for 20 min on a hot plate was performed. A layer dry film resist (DFR) Ordyl SY355 (Elga Europe, Milano, Italy) was laminated and soft baked at 85 °C for 5 min. This step was repeated according to the channel height that was required (each layer adding 50 µm). The exposure was carried out through a polymer film mask (Packaging laboratory, AVT, TU Dresden, Dresden, Germany) at an intensity of 1.66 $W \cdot cm^{-2}$. The exposure time for two layers of resist was 90 s, while three layers required 120 s. The post-exposure bake (PEB) was performed at 85 °C, 30 min for each layer of resist. The substrate was developed in the Ordyl developer and rinser (Ordyl Developer & Rinser, Elga Europe) for 6 min in each. The development was finished off with rinsing of isopropanol and de-ionized water. The process was completed with a hard bake at 120 °C for 1.5 h.

2.3.2. Chip Fabrication

For chip fabrication, 27.5 g of PDMS (Sylgard 184, Dow Corning, Midland, MI, USA) in a ratio of 10:1 was mixed with an electric stirrer for 5 min. It was then de-gased in a vacuum chamber for 45 min. The bubble-free PDMS was poured on top of the flow master creating a layer thickness of 4 mm. The PDMS was then cured in a convection oven at 60 °C for 2.0 h. The chip was peeled off the master mould and bonded via oxygen-plasma (at 50 W for 2 min) onto a glass substrate.

2.3.3. Droplet Experiment

The microfluidic chip for the droplet generation was fabricated as explained above with a channel height of 150 µm (three layers of DFR). For the continuous phase we used a mineral oil (SpectraSyn10, ExxonMobil, USA) with 3 wt % of surface detergent (Span80, Sigma-Aldrich, St. Louis, MO, USA). The discontinuous phase was de-ionized water. Figure S3 in the supplement provides an overview photograph of the experimental setup and Figure S4 holds detailed information about the droplet generating chip system.

3. Results

The assembly of our setup was straightforward and concluded at a cost of about €720. The analogue input as well as output clamps of the fieldbus support four channels, meaning that our system, as designed, can be advanced to four pressure sources total. To run the system, we developed a Python-based software facilitating a graphical user interface (GUI) for easier control and is discussed below. The software was tested on a Linux system running on a Raspberry Pi 2.0 (Raspberry Pi Foundation, Caldecote, UK) and on MacOS X (Apple Inc., Cupertino, CA, USA).

The characterization of the pumping capability of the pressure source was carried out by measuring the output pressure with an independent pressure sensor. The measured results from the pressure sensor were evaluated for accuracy, precision, noise and hysteresis properties. All properties are given in mbar. In order to get a better understanding of the quality of these properties, we performed the same measurement and analysis with a commercially available pressure pump for reference. The resulting graphs can be seen in Figure 3. Each row in the graphs shows a different property over the measurement range (0, ..., 1000 mbar), while the columns hold the results for varying hydraulic resistances of the supplied microfluidic systems. The first column presents the graphs for the measurements without load, while the graphs in column two, three and four display the measurements with the load from a microfluidic system. The graphs with the blue dots are the results of the DIY pump setup while the red squares indicate the results of the commercial pump. The solid lines for each color show the average value over the entire range. The average value over the entire

measuring range and the particular standard deviation is additionally noted in Table 1. The ideal value for all properties is 0 mbar, which is also noted in the graphs of Figure 3 by a solid black line.

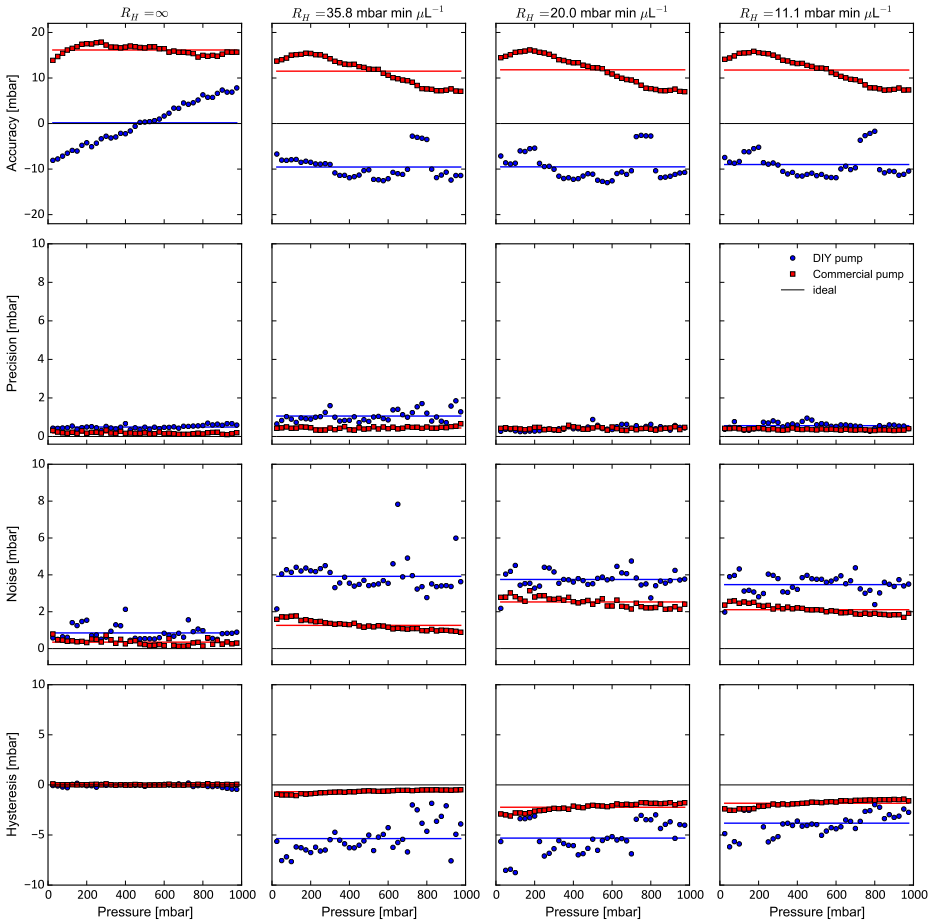

Figure 3. Characterization results of the commercial pump (**red** squares) and our DIY setup (**blue** dots) for both cases without load ($R_H = \infty$) and with load of a microfluidic system (R_H = 35.8, 20.0 and 11.0 mbar min μL^{-1}). Solid lines (**red** and **blue**) mark the average value over the entire pressure range. Evaluated over the rows are the pressure properties accuracy, precision, noise and hysteresis.

Table 1. Average value (mean) and standard deviation (STD) of the properties accuracy, precision, noise and hysteresis for both the DIY pressure source (DIY) and the commercial pressure pump (COMML) for varying hydraulic resistances over the entire pressure range.

		Accuracy		**Precision**		**Noise**		**Hysteresis**	
Unit:	R_H **mbar min** μL^{-1}	**Mean mbar**	**STD mbar**	**Mean mbar**	**STD mbar**	**Mean mbar**	**STD mbar**	**Mean mbar**	**STD mbar**
DIY	∞	0.16	4.81	0.49	0.09	0.85	0.38	−0.08	0.14
	35.8	−9.55	2.65	1.06	0.29	3.92	0.89	−5.36	1.53
	20.0	−9.51	3.03	0.43	0.13	3.75	0.46	−5.31	1.58
	11.0	−9.00	2.79	0.56	0.15	3.47	0.49	−3.82	1.11
Commercial	∞	16.15	0.98	0.18	0.05	0.35	0.16	0.02	0.03
	35.8	11.50	2.93	0.44	0.07	1.26	0.25	−0.68	0.17
	20.0	11.80	3.16	0.41	0.06	2.53	0.26	−2.23	0.39
	11.0	11.75	2.98	0.37	0.04	2.11	0.24	−1.83	0.34

3.1. DIY System Performance

3.1.1. Accuracy

Accuracy describes the difference between the measured value and the set nominal value and can be seen in row one of the graphs of Figure 3. Both pumps show a strong deviation in accuracy over all test conditions (without load as well as with load). The commercial pump outputs a positive offset pressure up to 16 mbar over the entire testing range. The deviation of this offset is rather small for the load free testing, while the test with load was higher due to a sine-like course of the offset. The DIY setup shows, with −9.5 mbar, a generally smaller deviation from the set value but a negative offset from the set value. The smallest offset from the set value in absolute is reached for the absence of load from 500 mbar to 600 mbar. The DIY pressure sources accuracy with a microfluidic system, as load is negative over the entire pressure range, giving out by tendency a value smaller than the required one. The deviation of the accuracy does not seem to be distributed systematically, but rather randomly.

3.1.2. Precision

Precision is the standard deviation over a series of measured values of an identical nominal value, describing the repeatability of the system showed in row two of Figure 3. The precision of both pumps for all testing cases (without load as well as with load) seems rather well and narrowly distributed, showing a high reproducibility of each pumping setup also for low hydraulic resistances. The data points are close to the x-axis and are almost ideal.

3.1.3. Noise

Noise is the standard deviation of a measured pressure value over time. This property determines the fluctuation of the pressure source during a quasi-static output. The noise of each pump in a quasi-static state can be seen in row three of Figure 3 and exhibits to be fairly low for no load, but increases with the load of a microfluidic system, where the pumps need to constantly re-adjust the pressure over the generated flow in the microfluidic networks. The noise of the commercial pump seems to increase with a decreasing hydraulic resistance, while the noise level of our setup seems to be generally at a higher level for the tests with load measurements. The deviation of the commercial pumps noise also seems to be more narrowly distributed.

3.1.4. Hysteresis

The measuring routine implemented a step function going up and down again within the pressure range. The measured value going up the step function and the measured value going down were compared. The difference was plotted over the pressure range for each set value and can be seen in row four of Figure 3. In the case of no load, both setups exhibit low hysteresis. The data points are close to the x-axis, and, therefore, to the ideal value. With decreasing hydraulic resistance from 35.8 to 20.0 mbar min μL^{-1}, the hysteresis of the commercial pump increases but then stagnates for 11.0 mbar min μL^{-1}. The standard deviation of the hysteresis seems to be systematically low. The DIY pressure setup generally displays a higher hysteresis with a higher deviation of the value as well.

3.2. DIY System GUI

The software to control the system includes a GUI for a straightforward use. The GUI, which is based on the Tkinter package (https://wiki.python.org/moin/TkInter), is shown in Figure 4. The interface provides control buttons for up to four channels allowing the conduction of complex experiments. The button controls allow an increase or decrease of fix values but also enable the setting to a specific value. Each channel is assigned a color, which can also be found as a continuous pressure graph over time in the middle canvas. The top row contains buttons for general functions such as a button for a snapshot of the graph, a save button for data, a button to assign pressures simultaneously,

or the "Zero" button to set off all controllers at once. The code is provided in the supplementary material. Within the classes of the pressure controller, we provide a series of more complex functions like sine, rectangular or ramp shape functions. An automation program to run the controllers can be written and accessed over the "Run Program" button. Every user is invited to add up to the software as user requirements may vary. The programmability is only limited by the language or the machine it is running on.

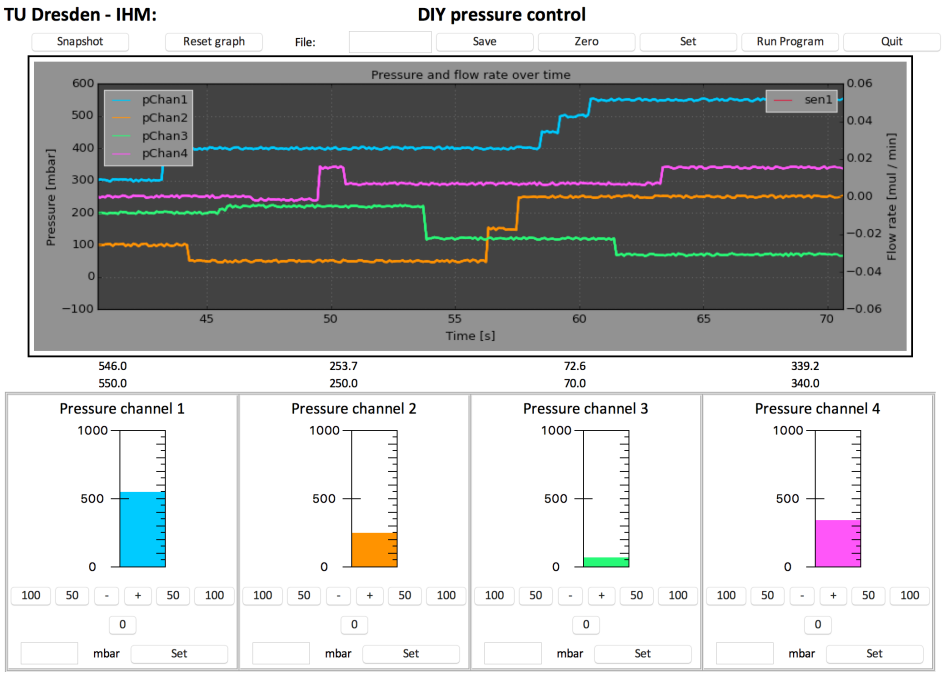

Figure 4. Graphical user interface (GUI) of the DIY system for controlling four pressure channels. (**Top**) general purpose buttons (Snapshot, Reset, Save, Set, Run Program, Quit); (**Middle**) canvas for pressure graphs over time; (**Bottom**) single channel control buttons with a visualization of the current set value.

3.3. Droplet Generation

A suitable field of application for such a system is droplet microfluidics. In a related experiment, we generated water in oil droplets using a flow focusing device, where two oil channels coming horizontally from the side pinch off a water phase coming in vertically. In the course of the experiment, we operated two pressure controllers independently setting various pressure ratios of the two phases (pressure oil—p_o; pressure water—p_w; ratio = p_o/p_w), resulting in different droplet sizes. The droplet volume over the pressure ratio is shown in Figure 5. For a better estimation, we fitted the data to a power function, which is also included in Figure 5. The data fit for the droplet volume V_d resulted in Equation (2) with a coefficient of determination R squared of $R^2 = 0.984$:

$$V_d\left(\frac{p_o}{p_w}\right) = 17.27\text{nl} \cdot \left(\frac{p_o}{p_w}\right)^{-1.577}. \quad (2)$$

The data as well as the fit show a decreasing of droplet volume with an increasing ratio p_o/p_w. With the setup, we were able to produce droplet volumes from 20 nL down to under 1 nL with a narrow size distribution. During the experiment, we observed the pressure controlled flow to be very quickly adjusting to a new operation point, which increased the throughput of the experimental settings. Preliminary experiments with regular syringe pumps exhibited a much slower response.

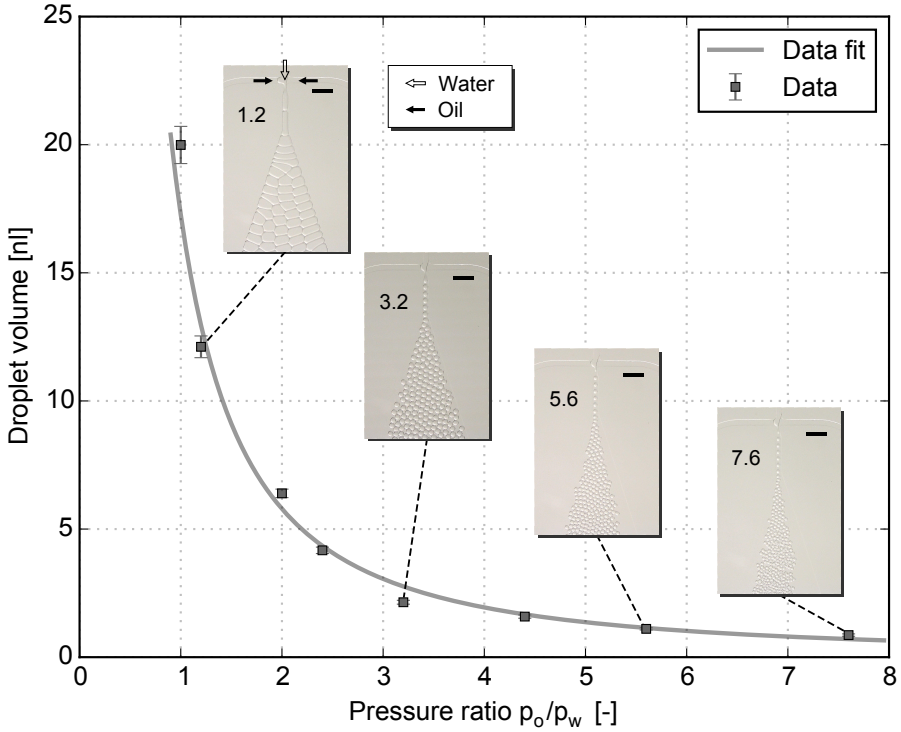

Figure 5. Droplet volume data and data fit over the pressure ratio p_o/p_w of the two pressure-driven phases. Additionally, data points were singled out showing a microscope image of the produced droplets. (scale bar = 500 µm).

4. Conclusions

The results show that the proposed DIY system is competitive in performance to the commercial pump system. Even though the commercial pump exhibits a slightly better quality in precision, noise and hysteresis, the results of our setup are still in a reasonable range. Especially when comparing the overall costs our pressure source seems very feasible with being under €1000, and, therefore under the commercial price by far, which lies in the range of a few thousands Euro. Table 2 makes a comparison between the DIY system and a typical commercially available system. The market offers both systems where the pressure is externally supplied, but also ones where the pressure is generated via an internal compressor. The systems with a built-in compressor allow a location-independent operation of the device while the system presented here, which is fed by an external pressure source, is bound to a location with a pressure outlet, although the external supply allows the use of other gases besides just air and each pressure controller can be supplied by a different type of gas. The developed Python-based software was able to run on both Linux and MacOS and is expected to work on Windows-based operating systems as well. The software developed allowed the implementation of a variety of functions, which are useful for front-end users and interesting for modification for developers. Most commercial software framework is strictly bound to Windows systems and is not as transparent, rarely leaving room for customization. The modular concept in combination with the software allows flexible customization of the pressure source. Components can be easily added or exchanged to adjust the functionality specific to an application. The straightforward concept assures also easy maintenance of the setup.

Table 2. Feature comparison between the DIY pump to a basic-equipped, commercially available pump systems.

Feature	DIY Pump	Commercial Pump
Pressure supply	external	build-in/external
External equipment	fieldbus system	none
Channels	1 (+3)	1
Manual control	no	yes
Operating system	MacOS, Linux, Windows	Windows
Software	open-source	corporate
Usability	front-end user/developer	front-end user

4.1. Fields of Applications

As we demonstrated, the DIY system is applicable and very well suitable in the generation of droplets. The system operates fast and can be regulated to a precise degree. The application we presented can be used for a droplet-based micro cultivation or particle synthesis, although the capability of a programmable pressure source is not limited to a pumping device as presented here. The pressure source is also beneficial for a precise pressure control of pneumatic membrane valves. The pressure source can easily be connected via quick-lock coupling to external solenoid valves. These solenoid valves feed integrated on-chip membrane valves and can be operated at an optimal pressure. A further field of application lies in a testbench setup for destructive de-lamination tests for microfluidic chip bonding. The bonding of microfluidic systems is always critical and therefore of special interest [20,21]. To test such a bond, the system's outlet is blocked, while at the inlet, a pressured is applied, which is increased until the chip ruptures. The bonding typically withstands pressures of over 1 bar and more. In order to increase the capability of the pressure source, the pressure controller can be exchanged with a model, allowing a maximum pressure of up to 9 bar. The external supply of the pressure source allows the use of any desired gas. The system can be used this way, purging with inert gas to moderate either a chemical reaction, e.g., during emulsion polymerization, or to incubate microbial organisms on a microfluidic chip.

4.2. Costs

The proposed setup is a total cost of €720, only a fraction of the price of the commercially available systems. The fieldbus system we used is rather sophisticated and could be replaced by a microcontroller system e.g., Arduino (Arduino S.r.l., Genova, Italy) to reduce the overall costs even further. However, the Arduino Uno e.g., does not support an analogue output signal. In order to achieve the output functionality, an additional digital-analog-converter (DAC) shield ought to be implemented. The implementation of an Arduino system would increase accessibility following the open-hardware idea. Another way to go is to expand the described system since the fieldbus system used additionally supports another three pressure controllers to build up a four-channel pressure source. The additional costs would only be the price of the pressure controllers, which are €250 (VAT excl.) each. The ability to run on the Raspberry Pi 2 is beneficial to reduce the costs of the system further.

Supplementary Materials: Supplementary materials can be found at http://www.mdpi.com/2411-5134/1/2/13/s1.

Acknowledgments: We gratefully thank the German Research Foundation Research Training Group 1865 "Hydrogel-Based Microsystems" and the Center for Advancing Electronics Dresden (cfaed) for financial support.

Author Contributions: Philipp Frank and Sebastian Haefner conceived and designed the experiments; Philipp Frank performed the experiments; Philipp Frank, Martin Elstner and Andreas Richter analyzed the data; Sebastian Haefner contributed reagents/materials/analysis tools; Philipp Frank wrote the paper.

Conflicts of Interest: The authors declare no conflict of interest.

Abbreviations

The following abbreviations are used in this manuscript:

DIY: Do It Yourself
DFR: Dry Film Resist

References

1. Schulte, T.H.; Bardell, R.L.; Weigl, B.H. Microfluidic technologies in clinical diagnostics. *Clin. Chim. Aacta* **2002**, *321*, 1–10.
2. Breslauer, D.N.; Lee, P.J.; Lee, L.P. Microfluidics-based systems biology. *Mol. Biosyst.* **2006**, *2*, 97–112.
3. Yager, P.; Edwards, T.; Fu, E.; Helton, K.; Nelson, K.; Tam, M.R.; Weigl, B.H. Microfluidic diagnostic technologies for global public health. *Nature* **2006**, *442*, 412–418.
4. Feng, X.; Du, W.; Luo, Q.; Liu, B.F. Microfluidic chip: Next-generation platform for systems biology. *Anal. Chim. Aacta* **2009**, *650*, 83–97.
5. Salieb-Beugelaar, G.B.; Simone, G.; Arora, A.; Philippi, A.; Manz, A. Latest developments in microfluidic cell biology and analysis systems. *Anal. Chem.* **2010**, *82*, 4848–4864.
6. Xia, Y.N.; Whitesides, G.M. Soft lithography. *Annu. Rev. Mater. Sci.* **1998**, *37*, 551–575.
7. Kim, P.; Kwon, K.W.; Park, M.C.; Lee, S.H.; Kim, S.M.; Suh, K.Y. Soft lithography for microfluidics: A review. *Biochip J.* **2008** *2*, 1–11.
8. Unger, M.A.; Chou, H.P.; Thorsen, T.; Scherer, A.; Quake, S.R. Monolithic microfabricated valves and pumps by multilayer soft lithography. *Science* **2000**, *288*, 113–116.
9. Fordyce, P.M.; Diaz-Botia, C.A.; DeRisi, J.L.; Gomez-Sjoberg, R. Systematic characterization of feature dimensions and closing pressures for microfluidic valves produced via photoresist reflow. *Lab Chip* **2012**, *12*, 4287–4295.
10. Frank, P.; Haefner, S.; Paschew, G.; Richter, A. Rounding of negative dry film resist by diffusive backside exposure creating rounded channels for pneumatic membrane valves. *Micromachines* **2015**, *6*, 1588–1596.
11. Duffy, D.C.; McDonald, J.C.; Schueller, O.J.A.; Whitesides, G.M. Rapid prototyping of microfluidic systems in poly(dimethylsiloxane). *Anal. Chem.* **1998**, *70*, 4974–4984.
12. Vulto, P.; Glade, N.; Altomare, L.; Bablet, J.; Tin, L.D.; Medoro, G.; Chartier, I.; Manaresi, N.; Tartagni, M.; Guerrieri, R. Microfluidic channel fabrication in dry film resist for production and prototyping of hybrid chips. *Lab Chip* **2005**, *5*, 158–162.
13. Paul, D.; Pallandre, A.; Miserere, S.; Weber, J.; Viovy, J.L. Lamination-based rapid prototyping of microfluidic devices using flexible thermoplastic substrates. *Electrophoresis* **2007**, *28*, 1115–1122.
14. Stephan, K.; Pittet, P.; Renaud, L.; Kleimann, P.; Morin, P.; Ouaini, N.; Ferrigno, R. Fast prototyping using a dry film photoresist: Microfabrication of soft-lithography masters for microfluidic structures. *J. Micromech. Microeng.* **2007**, *17*, N69–N74.
15. Takao, H.; Ishida, M. Microfluidic integrated circuits for signal processing using analogous relationship between pneumatic microvalve and MOSFET. *J. Microelectromech. Syst.* **2003**, *12*, 497–505.
16. Oh, K.W.; Lee, K.; Ahn, B.; Furlani, E.P. Design of pressure-driven microfluidic networks using electric circuit analogy. *Lab Chip* **2012**, *12*, 515.
17. Perdigones, F.A.; Luque, A.; Quero, J.M. Correspondence between electronics and fluids in mems: Designing microfluidic systems using electronics. *IEEE Trans. Ind. Electron.* **2014**, *8*, 6–17.
18. Wijnen, B.; Hunt, E.J.; Anzalone, G.C.; Pearce, J.M. Open-source syringe pump library. *PLoS ONE* **2014**, *9*, e107216.
19. Damase, T.R.; Stephens, D.; Spencer, A.; Allen, P.B. Open source and DIY hardware for DNA nanotechnology labs. *J. Biol. Methods* **2015**, *2*, e24.
20. Hong, S.M.; Kim, S.H.; Kim.; H.J.; Hwang, H.I. Hydrophilic surface modification of PDMS using atmospheric RF plasma. *J. Phys. Conf. Ser.* **2006**, *34*, 656–661.

21. Thompson, C.S.; Abate, A.R. Adhesive-based bonding technique for PDMS microfluidic devices. *Lab Chip* **2013**, *13*, 632.